

# Ca<sub>7</sub>Si<sub>2</sub>P<sub>2</sub>O<sub>16</sub>:Eu<sup>2+</sup> green phosphor for optic enhancement of the WLEDs dual-layer remote structure

Van Liem Bui<sup>1</sup>, Guo-Feng Luo<sup>2</sup>, Tam Nguyen Kieu<sup>3</sup>

<sup>1</sup>Faculty of Fundamental Science, Industrial University of Ho Chi Minh City, Ho Chi Minh City, Vietnam

<sup>2</sup>Department of Electrical Engineering, National Kaohsiung University of Science and Technology, Taiwan

<sup>3</sup>Faculty of Electrical and Electronics Engineering, Ton Duc Thang University, Ho Chi Minh City, Vietnam

## Article Info

### Article history:

Received Aug 2, 2021

Revised Apr 19, 2022

Accepted Jun 1, 2022

### Keywords:

Ca<sub>7</sub>Si<sub>2</sub>P<sub>2</sub>O<sub>16</sub>:Eu<sup>2+</sup>

Color homogeneity

Luminous flux

Monte Carlo method

WLEDs

## ABSTRACT

To enhance the dual-layer remote phosphorus configuration's color standard help spread its application in the LED devices, the new green-emitting phosphor of Ca<sub>7</sub>Si<sub>2</sub>P<sub>2</sub>O<sub>16</sub>:Eu<sup>2+</sup> is proposed. The sol-gel method is used to dope the Eu<sup>2+</sup> ions with Ca<sub>7</sub>Si<sub>2</sub>P<sub>2</sub>O<sub>16</sub>. Increasing the ion Eu<sup>2+</sup> concentration can lead to high thermal stability, color-tunable ability, stronger green emission band, and higher photoluminescence extraction. The dual-layer structure's color standards, as well as the luminous flux, are examined with different concentrations of Ca<sub>7</sub>Si<sub>2</sub>P<sub>2</sub>O<sub>16</sub>:Eu<sup>2+</sup> in the phosphor layer. Owing to the improved features, the green phosphor Ca<sub>7</sub>Si<sub>2</sub>P<sub>2</sub>O<sub>16</sub>:Eu<sup>2+</sup> has enhanced the emission intensity in the blue and green wavelengths, resulting in better color mixing and distribution. The luminescence shows the enhancement when increasing the concentration of Ca<sub>7</sub>Si<sub>2</sub>P<sub>2</sub>O<sub>16</sub>:Eu<sup>2+</sup>. However, the color rendering feature can present a reduction with more than 10% wt. green phosphor within the double-layer phosphorus remote configuration, due to color balance's loss.

This is an open access article under the [CC BY-SA](https://creativecommons.org/licenses/by-sa/4.0/) license.



## Corresponding Author:

Tam Nguyen Kieu

Faculty of Electrical and Electronics Engineering, Ton Duc Thang University

Ho Chi Minh City, Vietnam

Email: [nguyenkieu@tdtu.edu.vn](mailto:nguyenkieu@tdtu.edu.vn)

## 1. INTRODUCTION

Phosphors have been widely utilized in white lighting-emitting diodes (WLEDs) production. The Ca<sub>2</sub>Si<sub>2</sub>P<sub>2</sub>O<sub>16</sub> is a natural silicate phosphor that is somehow superior to the conventional sulfide phosphors in terms of light conversion performance, excitation spectra, and chemical stability. In addition to that, it is cost-efficiency as the raw ingredient for fabrication is affordable [1], [2]. Thus, Ca<sub>2</sub>Si<sub>2</sub>P<sub>2</sub>O<sub>16</sub> silicate phosphor is potential material for producing WLED with high efficiency. However, the application of this phosphor has not been thoroughly analyzed, and its performance was not excellent enough for the high-demand WLED market. Besides, analysis of Ca<sub>2</sub>Si<sub>2</sub>P<sub>2</sub>O<sub>16</sub> on the optical application is barely reported. Its use in the biological field was first demonstrated in the research of Chen *et al.* in 2012 [3]. It was shown that Ca<sub>2</sub>Si<sub>2</sub>P<sub>2</sub>O<sub>16</sub> is a potential biomaterial for the periodontal tissue regeneration aspect because it can help increase the periodontal ligament tissues as well as osteoblast/cementoblast-like tissue variation.

One of the favorite ion-doped phosphor materials in this lighting industry is the Eu<sup>2+</sup>-doped one since it has an excellent ability to absorb the blue-emitting LED chips then emit visible lights [4]-[6]. Moreover, Eu<sup>2+</sup>-doped phosphors possess efficient luminous performance and high stability thanks to the distorted coordination surrounding the Eu<sup>2+</sup> ions provided by the rigid frameworks with covalent Si-O bonds [7]-[9]. Thus, other studies mentioned other silicate phosphor doped with this Eu<sup>2+</sup> ion such as (Ba<sub>1-x</sub>Sr<sub>x</sub>)<sub>2</sub>SiO<sub>4</sub>:Eu<sup>2+</sup> with high red emission at 598 nm [10]-[13] Ca<sub>3</sub>SiO<sub>4</sub>Cl<sub>2</sub>:Eu<sup>2+</sup> with orange light emitted [14],

and  $\text{Sr}_5(\text{PO}_4)_2(\text{SiO}_4):\text{Eu}^{2+}$  generating green lights [15]. Hence, we decided to dope  $\text{Eu}^{2+}$  ion with silicate  $\text{Ca}_2\text{Si}_2\text{P}_2\text{O}_{16}$  phosphor host to enhance the efficiency of this phosphor. In addition to that, we will apply this  $\text{Ca}_2\text{Si}_2\text{P}_2\text{O}_{16}:\text{Eu}^{2+}$  to the double-layer remote phosphorus configuration with the aim of achieving better color uniformity as well as luminous efficacy of WLEDs. The preparation of doping  $\text{Eu}^{2+}$  ions into the  $\text{Ca}_2\text{Si}_2\text{P}_2\text{O}_{16}$  phosphor host is carried out with the sol-gel technique. The WLEDs modeling featuring double-layer remote configuration is designed with LightTools software and the Monte Carlo method. The luminescence properties, including the heat consistency as well as luminous efficiency of this phosphor, are examined and reported. Plus, the calculations of transfer energy and activation energy of this green-emitting phosphor are demonstrated. The color quality factor of dual-layer WLED, which is among the most critical objectives of the study, is also investigated with the presence of various concentrations of  $\text{Ca}_2\text{Si}_2\text{P}_2\text{O}_{16}:\text{Eu}^{2+}$ .

## 2. COMPUTATIONAL MODEL

### 2.1. The green-emitting phosphor $\text{Ca}_7\text{Si}_2\text{P}_2\text{O}_{16}:\text{Eu}^{2+}$ composing

The green-emitting phosphor  $\text{Ca}_7\text{Si}_2\text{P}_2\text{O}_{16}:\text{xEu}^{2+}$  with x from 0.01 to 0.07 is fabricated utilizing the sol-gel method. The chemical composition of this phosphor includes the calcium nitrate  $\text{Ca}(\text{NO}_3)_2 \cdot 4\text{H}_2\text{O}$ , tetraethyl silicate ( $\text{Si}(\text{OC}_2\text{H}_5)_4$ , TEOS),  $\text{NH}_4\text{H}_2\text{PO}_4$ ,  $\text{Eu}_2\text{O}_3$ , and chelating material – citric acid. It is possible to prepare of  $\text{Ca}_7\text{Si}_2\text{P}_2\text{O}_{16}:\text{xEu}^{2+}$  with  $\text{x}=0.05$  via creating three different solutions, then mixing and firing them under certain conditions [16].

The first solution (1) is prepared by slurring 0.2053 g of  $\text{Eu}_2\text{O}_3$  in diluted nitric acid  $\text{HNO}_3$ . It is then blended with  $\text{Ca}(\text{NO}_3)_2 \cdot 4\text{H}_2\text{O}$  (5.234 g) in a 99.5% citric acid liquid. After that, a stirring process is performed constantly at  $80^\circ\text{C}$  until obtaining the clear solution (1). Next, solution (2) is attained via a process of mixing 0.767 g  $\text{NH}_4\text{H}_2\text{PO}_4$  in deionized-water nitric acid. Specifically, the ratio of nitric acid to the ions is 2:1. In (3) solution is formed by blending 1.389 g TEOS, diluted  $\text{HNO}_3$ , and ethanol altogether, and finally hydrolyzing it using the stirring method in 20–40 minutes.

After obtaining the three solutions, the solutions will be mixed and stirred at room temperature for a few hours. Then to stimulate the metal citrates to polymerize, the ethylene glycol, with the ratio to the citric acid of 4:1, is added. After that, the mixture is gradually heated to  $100^\circ\text{C}$ , and fired at this temperature in the next 2 hours. Then, the product is taken out and placed in an oven for the drying process under  $100^\circ\text{C}$ – $150^\circ\text{C}$  for about 5–15 hours. After this process finishes, the attained product is porous solid resins that are treated under  $1000^\circ\text{C}$  lasting 8 hours in the air. Finally, the product is well-mixed and put into a covered carbon-integrated crucible for 10-hour firing at  $1300^\circ\text{C}$  [17].

### 2.2. Characterization of phosphor and simulation of the dual-layer WLED model

The attained  $\text{Ca}_7\text{Si}_2\text{P}_2\text{O}_{16}:\text{Eu}^{2+}$  has a broad range of absorption wavelengths of 300 – 450 nm, which implies that this green phosphor can absorb the UV-light and blue-light from LED chips (360 – 400 nm). It exhibits two wavelengths that peak at 520 nm and 650 nm with high emission intensity. Also, as the concentration of  $\text{Eu}^{2+}$  in the phosphor host increased, the red-shift in the spectral band presented a switch to the region of near-white color, from the yellowish-green one. The  $\text{Eu}^{2+}$  particles' conversion of energy is responsible for this color transition. The  $\text{Eu}^{2+}$  power conversion (from  $4f^7$  ground position to  $4f^65d^1$  excited position) is generally deducted from the transition energy of the free ion. The relation of this energy transfer can be demonstrated in P. Dorenbos' research [18]:

$$E_{em} = E_{free} - D - \Delta S \quad (1)$$

in which  $E_{free}$  describes the constant value of every lanthanide particle relative to the red-shift power of the free (gaseous) lanthanide particles. Meanwhile, D presents the red-shift deducted energy. The thermal-quenching activation energy  $\Delta E$  of the  $\text{Eu}^{2+}$  emission could be calculated using the modified formula of Arrhenius [19]-[22]:

$$I_T = \frac{I_0}{1 + c \exp(-(\Delta E/kT))} \quad (2)$$

Here,  $I_0$  indicates the prime emitting ferocity,  $I_T$  shows the severity at various temperature points,  $\Delta E$  describes the heat absorption's activation power, and  $c$  is fixed for a specific host, while  $k$  denotes the Boltzmann absolute ( $8.617 \times 10^{-5} \text{ eV K}^{-1}$ ). The calculated  $\Delta E$  was at about 0.222 eV, and the luminescent emission of this  $\text{Ca}_7\text{Si}_2\text{P}_2\text{O}_{16}:\text{Eu}^{2+}$  has high thermal stability. Thus, this phosphor is potentially used in the WLED package to attain tunable color and thermal steadiness features.

Phosphor layers used for the simulation of the WLED package are mainly comprised of the phosphor particles and silicone matrix. The flat phosphor-silicone layer is designed using the LightTools 9.0

software and the Monte Carlo experiment [23]-[25]. To manage to simulate the LED model, the beginning task will be defining the essential parts and structure them, then, the concentration of the used phosphor, which is  $\text{Ca}_7\text{Si}_2\text{P}_2\text{O}_{16}:\text{Eu}^{2+}$ , will be adjusted to examine its influences on the scattering, absorption, transmittance, and extraction of lights in the phosphor layers or the WLED package. The change in this green phosphor amount probably stimulates the fluctuation of yellow phosphor  $\text{YAG}:\text{Ce}^{3+}$  concentration, presented in more detail in the next section. The simulated WLEDs are investigated with the dual-layer structure featuring an 8500 K correlating color temperature (CCT). The actual WLED built with conformal phosphor coating method is demonstrated in Figure 1. The reflector of the WLED model is designed at 2.07 m, 8 mm, and 9.85 mm, in the height and the length of the bottom and top surfaces, respectively. The layer of yellow phosphor placed over LED chips is 0.08 mm thick. There are nine blue emitting LED chips attached to the reflectors cave. Each of them has a radiant flux of 1.16 W along with 453 nm optical wavelength, and 1.14 mm<sup>2</sup> x 0.15 mm in size (square base x height).



Figure 1. Photograph of WLEDs

### 3. RESULTS AND ANALYSIS

$\text{Ca}_7\text{Si}_2\text{P}_2\text{O}_{16}:\text{Eu}^{2+}$  concentration becoming higher causes the yellow phosphor concentration to decrease, as displayed in Figure 2. This trend sustains the stable CCT of the WLED during its operating hours. In addition to that, the reduction of the yellow phosphor percentage in the phosphor compound has significant effects on both the scattering and absorbing ability of the packages, from which the color uniformity and the optical extraction efficacy get remarkable results. Also, from Figure 2, the influence from the particle size of green phosphor  $\text{Ca}_7\text{Si}_2\text{P}_2\text{O}_{16}:\text{Eu}^{2+}$  is observed. The increasing size of this green particle would be proportional to the yellow phosphor's concentration. As can be seen, the highest  $\text{YAG}:\text{Ce}^{3+}$  concentration is at nearly 9% when 5%wt. and 20 $\mu\text{m}$  of  $\text{Ca}_7\text{Si}_2\text{P}_2\text{O}_{16}:\text{Eu}^{2+}$  are applied. Conversely, at the same particle size but higher concentration of green phosphor of 20%wt., the concentration of the yellow phosphor declines considerably to lower than 3%wt.

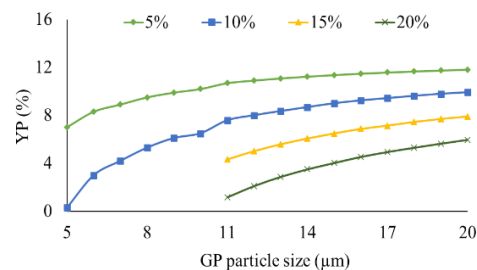


Figure 2. Modifying the phosphor's concentration to preserve the average CCT

The  $\text{Ca}_7\text{Si}_2\text{P}_2\text{O}_{16}:\text{Eu}^{2+}$  addition to the dual-layer WLED remote phosphorus package improves the lighting performance, as observed in Figure 3. Particularly, the spectral regions at 420 nm - 480 nm and 500 nm - 640 nm in the wavelengths (when the maximum sum powers are ~1 and ~0.4, respectively) show enhancements with the green  $\text{Ca}_7\text{Si}_2\text{P}_2\text{O}_{16}:\text{Eu}^{2+}$  phosphor presence, compared with the reference spectrum (the spectral regions at 380 nm - 420 nm when there is no power). That leads to the improved luminous output of the WLED. Also, the enhancement in the spectral intensity of the blue wavelength implies that the

scattering of blue beams is boosted or the scattered lights in the phosphor structures are promoted. This probably results in more uniformity of WLED color distribution. Therefore, the green phosphor  $\text{Ca}_7\text{Si}_2\text{P}_2\text{O}_{16}:\text{Eu}^{2+}$  is able to manage the color quality of WLEDs even at high CCT, such as the 8500 K WLED structure in this study. The addition of  $\text{Ca}_7\text{Si}_2\text{P}_2\text{O}_{16}:\text{Eu}^{2+}$  benefits the luminous flux, which is displayed in Figure 4. As can be seen, when the amount of  $\text{Ca}_7\text{Si}_2\text{P}_2\text{O}_{16}:\text{Eu}^{2+}$  in the phosphor compounding increases from 2%wt. to 20%wt., the luminance flux becomes higher, regardless of the particle sizes (5% increase for particle sizes from 5 $\mu\text{m}$ , 10% increase for particle sizes from 8 $\mu\text{m}$ , 15% increase for particle sizes from 12 $\mu\text{m}$  and 20% increase for particle sizes from 17 $\mu\text{m}$ ). The luminous flux is getting better when compared to the initial data (just tiny increase percentages for particle sizes smaller than 5 $\mu\text{m}$ ).

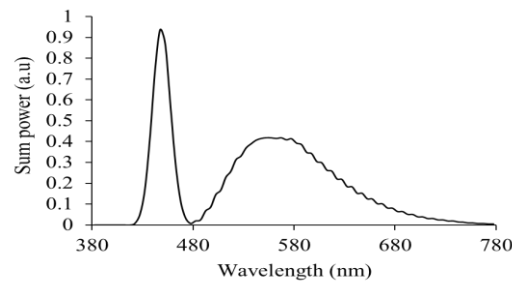


Figure 3.  $\text{Ca}_7\text{Si}_2\text{P}_2\text{O}_{16}:\text{Eu}^{2+}$  concentration functions as the 5000 K WLEDs emitting spectrum

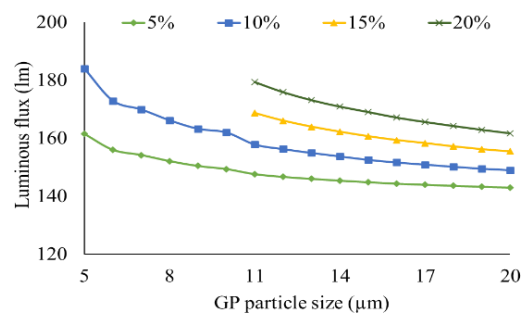


Figure 4.  $\text{Ca}_7\text{Si}_2\text{P}_2\text{O}_{16}:\text{Eu}^{2+}$  concentration functions as the WLEDs luminous flux

Generally, the improvement in the luminous flux would be in reversed proportion to the color quality of the phosphor-converted WLED. Thus, if the procedure of LED fabrication focuses on the enhancement of color harmony of white light, a certain reduction in luminous flux can be acceptable. This also indicates that the selection of phosphor  $\text{Ca}_7\text{Si}_2\text{P}_2\text{O}_{16}:\text{Eu}^{2+}$  concentration is necessary for controlling both color adequacy and lumen efficiency at high levels. The change in concentration of  $\text{Ca}_7\text{Si}_2\text{P}_2\text{O}_{16}:\text{Eu}^{2+}$  green phosphor does impact the chromatic properties of white lights, which is illustrated from Figure 5 to Figure 7.

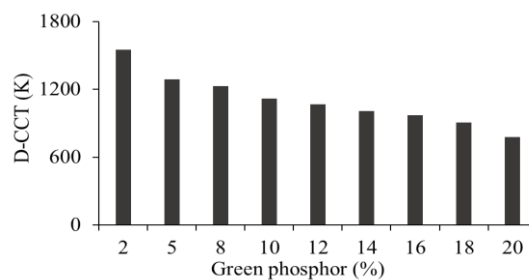


Figure 5.  $\text{Ca}_7\text{Si}_2\text{P}_2\text{O}_{16}:\text{Eu}^{2+}$  concentration functions as the WLEDs color deviation

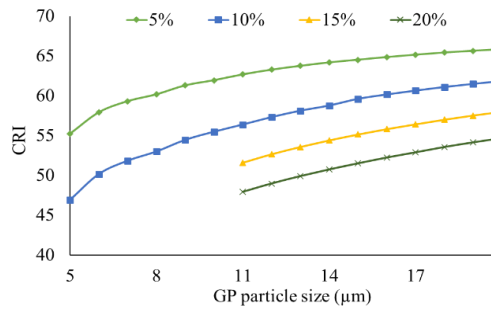


Figure 6.  $\text{Ca}_7\text{Si}_2\text{P}_2\text{O}_{16}:\text{Eu}^{2+}$  concentration functions as the WLEDs color rendering index

In Figure 5, the color deviation (D-CCT), one of the parameters to evaluate the chromatic homogeneity of the white light, decreases when the percentage of the green phosphor in the phosphorus layer increases. Compared to the D-CCT at 2% wt., when using 20% wt. of  $\text{Ca}_7\text{Si}_2\text{P}_2\text{O}_{16}:\text{Eu}^{2+}$ , this figure is reduced by approximately 500 K. The reduction in color variance results in better color uniformity. This benefit results from the enhanced scattering and absorption performance owing to the presence of the  $\text{Ca}_7\text{Si}_2\text{P}_2\text{O}_{16}:\text{Eu}^{2+}$  phosphor layer. As mentioned above, the scattering of blue lights is enhanced not only benefits the luminance flux but also stimulates color blending, leading to higher uniformity. Additionally, the absorption characteristic of this green phosphor allows it to absorb the blue and yellow emitting lights from blue chips allowing the phosphor layer to convert these lights into the green-light elements. Notably, the blue-light absorption of this  $\text{Ca}_7\text{Si}_2\text{P}_2\text{O}_{16}:\text{Eu}^{2+}$  is better than its yellow-light absorption. Therefore, the green emission becomes stronger, and more green beams are generated, which is beneficial to the color homogeneity metric of LED lights. Besides, the use of  $\text{Ca}_7\text{Si}_2\text{P}_2\text{O}_{16}:\text{Eu}^{2+}$  can offer cost-efficiency fabrication since it has a lower price than many other phosphor materials. Hence, the manufacturers can apply this green phosphor in large-scale production.

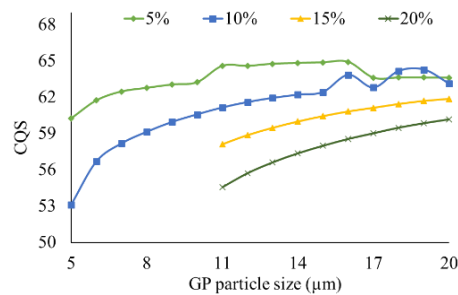


Figure 7.  $\text{Ca}_7\text{Si}_2\text{P}_2\text{O}_{16}:\text{Eu}^{2+}$  concentration functions as the WLEDs color quality scale

Besides color uniformity, two other important metrics should be analyzed when it comes to color-quality evaluation. The color rendering indices, which evaluate an item's color faithfulness revealed under a lighting source in comparison with the natural light, slightly decrease when there is a higher amount of  $\text{Ca}_7\text{Si}_2\text{P}_2\text{O}_{16}:\text{Eu}^{2+}$  in the phosphor film, demonstrated in Figure 6. This is probably attributed to the color imbalance caused by the green-light dominance. Particularly, the excessive rise of the  $\text{Ca}_7\text{Si}_2\text{P}_2\text{O}_{16}:\text{Eu}^{2+}$  concentration leads to the redundancy in the green color element, which is higher than the blue and yellow color ones and thus degrading the chromatic fidelity of the WLED light. However, this insignificant reduction in CRI would become accepted as CRI is somehow not an overall index of chromatic assessment. Recent studies have pointed out that CRI is a factor of another metric of color evaluation, the CQS. It includes two other factors, besides the CRI, the visual preference of the human, and the color coordinate. Thus, the CQS is considered the best parameter to examine the color quality of a light source. As in Figure 7, the CQS increases with the rise of the  $\text{Ca}_7\text{Si}_2\text{P}_2\text{O}_{16}:\text{Eu}^{2+}$  concentration from 2% wt. to 10% wt. More than 10% wt.  $\text{Ca}_7\text{Si}_2\text{P}_2\text{O}_{16}:\text{Eu}^{2+}$  will result in the reduction of both CRI and CQS due to the influence from the redundant green-color element. To obtain high and consistent CRI and CQS, the appropriate amount of green phosphor is suggested to be defined properly, for example, below 10% wt.

#### 4. CONCLUSION

The paper proposes  $\text{Ca}_7\text{Si}_2\text{P}_2\text{O}_{16}:\text{Eu}^{2+}$  as a new phosphor material for the dual-layer remote WLED structure to enhance its color quality and luminous efficacy.  $\text{Ca}_7\text{Si}_2\text{P}_2\text{O}_{16}$  is doped with ion  $\text{Eu}^{2+}$  using the chemical sol-gel technique. This phosphor has a broadband of absorption (300 – 450 nm), leading to the ability to be compatible with the near-UV-chip light emission. The  $\text{Eu}^{2+}$ -doped concentration dramatically affects the light features in this phosphor.  $\text{Ca}_7\text{Si}_2\text{P}_2\text{O}_{16}:\text{Eu}^{2+}$  performs high luminescent thermal stability, and two peak wavelengths of 520 and 650 nm with high emission energy. After increasing the green phosphor  $\text{Ca}_7\text{Si}_2\text{P}_2\text{O}_{16}:\text{Eu}^{2+}$  concentration to 20% wt., the green-emitting phosphor  $\text{Ca}_7\text{Si}_2\text{P}_2\text{O}_{16}:\text{Eu}^{2+}$  would raise the luminous efficiency substantially when placed in the double-layer configuration. It is possible to improve the color uniformity via raising  $\text{Ca}_7\text{Si}_2\text{P}_2\text{O}_{16}:\text{Eu}^{2+}$  amount since the higher the phosphor concentration is, the more the color deviation is reduced, and the higher the chromatic homogeneity becomes. As the green phosphorous concentration is fewer than 10% wt., the double-layer configuration CRI and CQS show stability and enhancement. A higher concentration (> 10% wt.) of  $\text{Ca}_7\text{Si}_2\text{P}_2\text{O}_{16}:\text{Eu}^{2+}$  probably reduces the color quality owing to the color imbalance caused by the excessive green light components in the package. Hence, identifying the proper  $\text{Ca}_7\text{Si}_2\text{P}_2\text{O}_{16}:\text{Eu}^{2+}$  concentration is critical, based on the needs and objectives of the WLED producers.





#### REFERENCES

- [1] S. Kumar, M. Mahadevappa, and P. K. Dutta, "Extended light-source-based lensless microscopy using constrained and regularized reconstruction," *Appl. Opt.*, vol. 58, no. 3, pp. 509-516, 2019, doi: 10.1364/AO.58.000509.
- [2] V. Su and C. C. Gao, "Remote GaN metalens applied to white light-emitting diodes," *Opt. Express*, vol. 28, pp. 38883-38891, 2020, doi: 10.1364/OE.411525.
- [3] F. -B. Chen, K. -L. Chi, W. -Y. Yen, J. -K. Sheu, M. -L. Lee and J. -W. Shi, "Investigation on Modulation Speed of Photon-Recycling White Light-Emitting Diodes With Vertical-Conduction Structure," *J. Lightwave Technol.*, vol. 37, no. 4, pp. 1225-1230, 15 Feb.15, 2019, doi: 10.1109/JLT.2018.2890331.
- [4] S. Xu *et al.*, "Exploration of yellow-emitting phosphors for white LEDs from natural resources," *Appl. Opt.*, vol. 60, no. 16, pp. 4716-4722, 2021, doi: 10.1364/AO.424108.
- [5] F. Jiang *et al.*, "Efficient InGaN-based yellow-light-emitting diodes," *Photon. Res.*, vol. 7, no. 2, pp. 144-148, 2019, doi: 10.1364/PRJ.7.000144.
- [6] S. Keshri *et al.*, "Stacked volume holographic gratings for extending the operational wavelength range in LED and solar applications," *Appl. Opt.*, vol. 59, no. 8, pp. 2569-2579, 2020, doi: 10.1364/AO.383577.
- [7] X. Xi *et al.*, "Chip-level Ce:GdYAG ceramic phosphors with excellent chromaticity parameters for high-brightness white LED device," *Opt. Express*, vol. 29, no. 8, pp. 11938-11946, 2021, doi: 10.1364/OE.416486.
- [8] H. S. El-Ghoroury, Y. Nakajima, M. Yeh, E. Liang, C. L. Chuang, and J. C. Chen, "Color temperature tunable white light based on monolithic color-tunable light emitting diodes," *Opt. Express*, vol. 28, no. 2, pp. 1206-1215, 2020, doi: 10.1364/OE.375320.
- [9] Z. Zhao, H. Zhang, S. Liu, and X. Wang, "Effective freeform TIR lens designed for LEDs with high angular color uniformity," *Applied Optics*, vol. 57, no. 15, pp. 4216-4221, 2018, doi: 10.1364/AO.57.004216.
- [10] H. Yu, G. Y. Cao, J. H. Zhang, Y. Yang, W. L. Sun, L. P. Wang, and N. Y. Zou, "Solar spectrum matching with white OLED and monochromatic LEDs," *Applied Optics*, vol. 57, no. 10, pp. 2659-2666, 2018, doi: 10.1364/AO.57.002659.
- [11] N. Anous, T. Ramadan, M. Abdallah, K. Qaraqa, and D. Khalil, "Impact of blue filtering on effective modulation bandwidth and wide-angle operation in white LED-based VLC systems," *OSA Continuum*, vol. 1, no. 3, pp. 910-929, 2018, doi: 10.1364/OSAC.1.000910.
- [12] P. Zhu, H. Zhu, G. C. Adhikari, and S. Thapa, "Spectral optimization of white light from hybrid metal halide perovskites," *OSA Continuum*, vol. 2, no. 6, pp. 1880-1888, 2019, doi: 10.1364/OSAC.2.001880.
- [13] H. Yuce, T. Guner, S. Balci, and M. M. Demir, "Phosphor-based white LED by various glassy particles: control over luminous efficiency," *Opt. Lett.*, vol. 44, no. 3, pp. 479-482, 2019, doi: 10.1364/OL.44.000479.
- [14] G. Liu, W. Hou, M. Han, "Unambiguous Peak Recognition for a Silicon Fabry-Pérot Interferometric Temperature Sensor," *J. Lightwave Technol.*, vol 36, no. 10, pp. 1970-1978, 2018, doi: 10.1109/JLT.2018.2797202.
- [15] Hong-Liang Ke *et al.*, "Lumen degradation analysis of LED lamps based on the subsystem isolation method," *Appl. Opt.*, vol 57, no. 4, pp. 849-854, 2018, doi: 10.1364/AO.57.000849.
- [16] L. Xiao, C. Zhang, P. Zhong, and G. He, "Spectral optimization of phosphor-coated white LED for road lighting based on the mesopic limited luminous efficacy and IES color fidelity index," *Appl. Opt.*, vol 57, no. 4, pp. 931-936, 2018, doi: 10.1364/AO.57.000931.
- [17] H. Lee, S. Kim, J. Heo, and W. J. Chung, "Phosphor-in-glass with Nd-doped glass for a white LED with a wide color gamut," *Opt. Lett.*, vol 43, no. 4, pp. 627-630, 2018, doi: 10.1364/OL.43.000627.
- [18] A. Ullah *et al.*, "Household light source for potent photo-dynamic antimicrobial effect and wound healing in an infective animal model," *Biomed. Opt. Express*, vol 9, no. 3, pp. 1006-1019, 2018, doi: 10.1364/BOE.9.001006.
- [19] A. Keller, P. Bialecki, T. J. Wilhelm, and M. K. Vetter, "Diffuse reflectance spectroscopy of human liver tumor specimens - towards a tissue differentiating optical biopsy needle using light emitting diodes," *Biomed. Opt. Express*, vol 9, no. 3, pp. 1069-1081, 2018, doi: 10.1364/BOE.9.001069.
- [20] Y. Peng *et al.*, "Flexible fabrication of a patterned red phosphor layer on a YAG:Ce<sup>3+</sup> phosphor-in-glass for high-power WLEDs," *Opt. Mater. Express*, vol 8, no. 3, pp. 605-614, 2018, doi: 10.1364/OME.8.000605.
- [21] L. Duan and Z. Lei, "Wide color gamut display with white and emerald backlighting," *Appl. Opt.*, vol. 57, no. 6, pp. 1338-1344, 2018, doi: 10.1364/AO.57.001338.
- [22] H. P. Huang, M. Wei, and L. -C. Ou, "White appearance of a tablet display under different ambient lighting conditions," *Opt. Express*, vol 26, pp. 5018-5030, 2018, doi: 10.1364/OE.26.005018.
- [23] Z. Li, Y. Tang, J. Li, X. Ding, C. Yan, and B. Yu, "Effect of flip-chip height on the optical performance of conformal white-light-emitting diodes," *Opt. Lett.*, vol 43, no. 5, pp. 1015-1018, 2018, doi: 10.1364/OL.43.001015.





- [24] A. I. Alhassan *et al.*, "Development of high performance green c-plane III-nitride light-emitting diodes," *Opt. Express*, vol 26, no. 5, pp. 5591-5601, 2018, doi: 10.1364/OE.26.005591.
- [25] S. Jost, C. Cauwerts, and P. Avouac, "CIE 2017 color fidelity index Rf: a better index to predict perceived color difference?," *J. Opt. Soc. Am. A*, vol 35, pp. B202-B213, 2018, doi: 10.1364/JOSAA.35.00B202.

## BIOGRAPHIES OF AUTHORS







**Van Liem Bui**     received a Bachelor of Mathematical Analysis and master's in mathematical Optimization, Ho Chi Minh City University of Natural Sciences, VietNam. Currently, He is a lecturer at the Faculty of Fundamental Science, Industrial University of Ho Chi Minh City, Viet Nam. His research interests are mathematical physics. He can be contacted at email: buivanliem@iuh.edu.vn.



**Guo-Feng Luo**     was born in Tainan city, Taiwan. He has been working at the Department of Electrical Engineering, National Kaohsiung University of Science and Technology, Kaohsiung, Taiwan. His research interest is optical material. He can be contacted at email: paradisefall02@gmail.com.



**Tam Nguyen Kieu**     was born in Phu Yen Province, Viet nam. He received his M.Sc. from university of transport and communications, Viet Nam in 2012 and defended his PhD. diploma at VSB-Technical University of Ostrava, Czech Republic. His research interests include the wireless communication, WiMax, energy harvesting, and MEC. He can be contacted at email: nguyenkietam@tdtu.edu.vn.